

2009

# Combining Remote Sensing Data and an Inundation Model to Map Tidal Mudflat Regions and Improve Flood Predictions: A Proof of Concept Demonstration in Cook Inlet, Alaska

Tal Ezer

Old Dominion University, tezer@odu.edu

Hua Liu

Old Dominion University, hxliu@odu.edu

Follow this and additional works at: [https://digitalcommons.odu.edu/ccpo\\_pubs](https://digitalcommons.odu.edu/ccpo_pubs)

 Part of the [Climate Commons](#), [Meteorology Commons](#), and the [Oceanography Commons](#)

## Repository Citation

Ezer, Tal and Liu, Hua, "Combining Remote Sensing Data and an Inundation Model to Map Tidal Mudflat Regions and Improve Flood Predictions: A Proof of Concept Demonstration in Cook Inlet, Alaska" (2009). *CCPO Publications*. 109.  
[https://digitalcommons.odu.edu/ccpo\\_pubs/109](https://digitalcommons.odu.edu/ccpo_pubs/109)

## Original Publication Citation

Ezer, T., & Liu, H. (2009). Combining remote sensing data and an inundation model to map tidal mudflat regions and improve flood predictions: A proof of concept demonstration in Cook Inlet, Alaska. *Geophysical Research Letters*, 36, 1-6. doi: 10.1029/2008gl036873

# Combining remote sensing data and an inundation model to map tidal mudflat regions and improve flood predictions: A proof of concept demonstration in Cook Inlet, Alaska

Tal Ezer<sup>1,2</sup> and Hua Liu<sup>3</sup>

Received 2 December 2008; revised 15 January 2009; accepted 22 January 2009; published 20 February 2009.

[1] Accurate flood predictions require high resolution inundation numerical models and detailed coastal and land topography data. However, such data are not always available. A new method to obtain topographic information of flood zones from remote sensing data is demonstrated here for Cook Inlet, Alaska, where tidal range reaches 8–10 m. The moving shoreline is detected from analysis of water coverage in satellite images taken at different tidal stages, and then the shoreline data from different times are combined with water level data from observations and models to produce new topographic maps of previously unobserved mudflats. The remote sensing-based analysis provides for the first time a way to evaluate the flood predictions of the inundation model of the inlet. The new flood-zone topography obtained from the remote sensing data will help to construct a more accurate inundation model in the future.

**Citation:** Ezer, T., and H. Liu (2009), Combining remote sensing data and an inundation model to map tidal mudflat regions and improve flood predictions: A proof of concept demonstration in Cook Inlet, Alaska, *Geophys. Res. Lett.*, 36, L04605, doi:10.1029/2008GL036873.

## 1. Introduction

[2] Accurate predictions of floods due to storm surges (e.g., the flooding of New Orleans by hurricane Katrina in August, 2005) or tsunamis (e.g., the destruction caused by the Indian Ocean tsunami in December, 2004) require high resolution inundation models [e.g., *Kowalik et al.*, 2006] and detailed near shore and land topographies. Very high resolution ( $\sim 1$  m) flood-inundation maps from airborne LiDAR data can be very useful [e.g., *Zhou*, 2009], but these data are costly and not easily available everywhere on the globe. Therefore, one may wonder if lower resolution, publicly available, satellite images can be used instead.

[3] The motivation for this study came about from three-dimensional model simulations (Figure 1) of tidal-driven floods in a sub-arctic estuary, Cook Inlet, Alaska [*Oey et al.*, 2007; *Ezer et al.*, 2008]. The large semi-diurnal tide (8–10 m range) in the inlet floods and exposes extensive mudflat regions (tens of square kilometers) twice daily, but lack of data on the morphology and topography of the mudflat

regions makes it difficult to accurately simulate the tidal flood or evaluate the inundation model. The topography data used by the model in these flood areas (magenta color in Figure 1) were based only on a subjective guess from various maps and charts. The model resolution ( $\sim 0.5$  km in the upper inlet) is insufficient to describe the various narrow channels in the inlet, but increasing the model resolution would not be practical without having high resolution topography data.

[4] Unlike the unpredictable nature of hurricanes and tsunamis and the difficulty of getting timely data during catastrophic events, the daily tides provide plenty of flood data to test inundation models. The value of remote sensing data from two platforms, Landsat Thematic Mapper (TM) and Enhanced Thematic Mapper (ETM+) and Moderate Resolution Imaging Spectroradiometer (MODIS), were tested for their usefulness to improve model topography and evaluate flood predictions. The idea is quite simple: (a) find satellite images at different times (and different tidal stages), (b) match each image with observed or model sea level, (c) find the shoreline contours separating water and land areas, (d) combine the shoreline and sea level data to produce new topography maps, (e) use the data to evaluate the model flood prediction, and (f) eventually use the new topography in new high resolution numerical models. In this study we evaluated the feasibility of steps (a)–(d) using sample data and started preliminary evaluation of step (e); if the results demonstrate the feasibility of the proposed approach (as we believe they did), one can proceed to step (f), using additional remote sensing data.

## 2. Methodology and Remote Sensing Data Processing

[5] Remote sensing and geographical information systems (GIS) have been used extensively for monitoring water resources, for example, to assess water clarity of lakes in Minnesota using Landsat [*Olmanson et al.*, 2008]. MODIS data were applied, for example, to monitor red tide in southwestern Florida coastal waters [*Hu et al.*, 2005]. Here, Landsat and MODIS data will be evaluated for a different purpose than their usual usage, to map a moving tidal-driven shoreline. The idea of using MODIS data to improve model inundation predictions has been originally mentioned by *Oey et al.* [2007], but here a higher resolution Landsat data is added and more quantitative analysis is conducted.

[6] The data used here include a total of six Landsat images and four Terra MODIS datasets (Tables 1 and 2). It was important to find not only a reliable good images, but also ones taken at different tidal stages (i.e., with different water coverage in each image). Figure 2 is an example of Landsat images at low and high water levels, showing the

<sup>1</sup>Center for Coastal Physical Oceanography, Old Dominion University, Norfolk, Virginia, USA.

<sup>2</sup>Virginia Modeling, Analysis and Simulation Center, Suffolk, Virginia, USA.

<sup>3</sup>Department of Political Science and Geography, Old Dominion University, Norfolk, Virginia, USA.

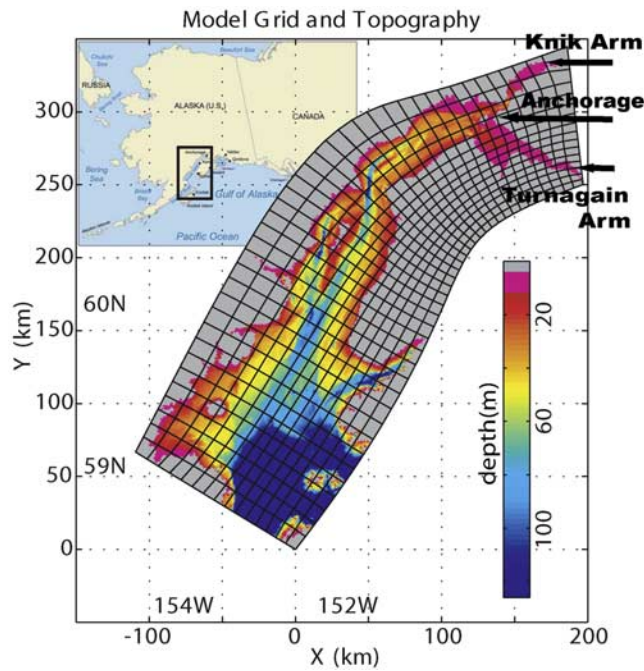


**Figure 1.** The curvilinear model grid (every 10th grid point is plotted) for Cook Inlet, Alaska, and bottom topography (depth in m relative to model maximum sea level). Gray color represents the land area that is never flooded in the model and magenta color represents wetting and drying regions that can be either water covered or exposed land cells in the model. The inset shows a map of the Gulf of Alaska and the modeled region (indicated by the box). The north-east upper inlet area around Anchorage is the focus of this study.

expansion of water coverage; it also demonstrates the difficulty of discriminating between water and land in this complex-topography region. Note that at this high latitude region, only ice-free summer images can be used. Landsat datasets include one Landsat TM image and five Landsat

**Table 1.** Spatial and Temporal Resolutions of Landsat and Terra MODIS Images

Satellite/Sensor	Spatial Resolution (m)	Temporal Resolution (days)
Landsat TM	Spectral bands 1–5 & 7: 30 m, Spectral band 6: 120 m	16
Landsat ETM+	Spectral bands 1–5 & 7: 30 m, Spectral band 6: 60 m	16
Terra MODIS	Spectral bands 1–2: 250 m, Spectral bands 3–7: 500 m, Spectral bands 8–36: 1000 m	1–2

ETM+ datasets (both datasets are 7-band multispectral images). MODIS image is a low-resolution hyperspectral dataset with various resolutions in different spectral bands. (See Table 1 for spatial and temporal resolutions).

[7] All the remote sensing data were imported to ERDAS IMAGINE, popular remote sensing data processing software. The initial projection was Albers Conical Equal Area projection for Landsat images and World Sinusoidal projection for MODIS images. The acquired images were rectified to the 1984 *Universal Transverse Mercator* zone 6N, at an accuracy of less than half a pixel. (Note that plots of satellite and model data in Figures 3 and 5, discussed later, used a coordinates with approximately equal distance in km for x and y). Unsupervised classification method and Gaussian Maximum Likelihood Classifier were chosen to classify the images into three categories: water, wetlands, and others. The color aerial photo of Anchorage was obtained from Geographic Information Network of Alaska and was used as reference in image classification. All the pixels in MODIS images were interpolated to a 30 × 30 m grid after image classification to match the pixels of the Landsat images. In order to derive the shoreline in each image, classified images were recoded to remove all terrestrial features and create water-only images. Longitude/latitudes of water pixels were stored for each water-only image. All the water-only images were then converted to vector data using GIS software ArcGIS. All the shorelines derived were stored as polygons in shape files.

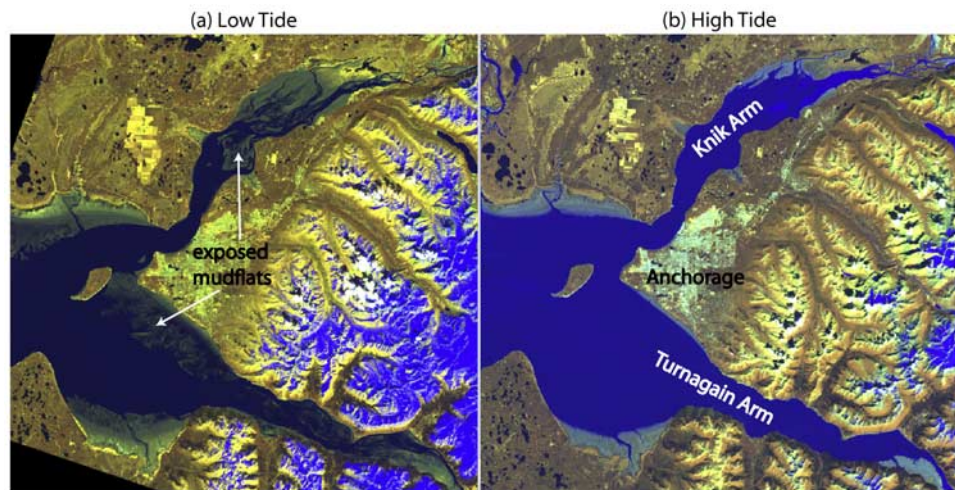


**Figure 2.** Landsat images of the upper Cook Inlet; dark blue represents water covered areas and light green/blue at the edges of the inlet represents exposed land or wet mudflats. (a) June 2, 2001, about one hour after minimum sea level was observed in Anchorage. (b) July 30, 2002, about one hour after maximum sea level was observed in Anchorage. Note that the two images use the same false color composite (Band 5 in red, Band 6 in green, and Band 1 in blue), but their colors appear slightly different due to the different spectral reflectance during the two dates and time of day.

**Table 2.** Remote Sensing Data Used in the Study

Acquisition Data and Time (GMT)	Sensor	Anchorage Sea Level (m)	Tidal Stage
07-10-1989, 20:47:19	Landsat-4/TM	1.33991	One hour after maximum sea level
04-28-2000, 20:59:56	Landsat-7/ETM+	1.15098	Two hours before maximum sea level
08-09-2000, 21:04:53	Landsat-7/ETM+	-0.81110	Three hours after minimum sea level
06-02-2001, 20:57:20	Landsat-7/ETM+	-3.37131	One hour after minimum sea level
05-20-2002, 20:56:06	Landsat-7/ETM+	2.15776	One hour before maximum sea level
07-30-2002, 21:01:49	Landsat-7/ETM+	1.29740	One hour after maximum sea level
05-01-2000, 20:50:19	Terra MODIS	-3.62775	One hour after minimum sea level
06-05-2001, 20:43:21	Terra MODIS	-4.44841	One hour before minimum sea level
05-21-2002, 20:48:17	Terra MODIS	0.74578	Three hours before maximum sea level
08-02-2002, 20:41:56	Terra MODIS	0.38088	Three hours before maximum sea level

[8] Since there is only one tide gauge in the upper inlet, near Anchorage, it was used as a reference to indicate the tidal stage at the time each image was obtained (Table 2). Note that during flood it may take the high water (including the tidal bore observed in the Turnagain Arm) 1–2 hours to travel from the Anchorage area and reach all the way to the farthest ends of the inlet [Oey *et al.*, 2007]. Spatial variations within the inlet will be taken into account in a follow-up study when the model dynamics is fully incorporated with the remote sensing data. In the preliminary study here, this time delay is not crucial, since quantitative matching of water level with remote sensing-based shoreline is only demonstrated near Anchorage where the spatial variations are negligible compared with the large tidal range.

### 3. Results

[9] Considering the temporal variations in the tidal dynamics in Cook Inlet (rapid sea level changes within each hour) and the spatial scales of topography (order of a few meters), the temporal and spatial scales of the remote sensing data (Table 1) clearly pose a great challenge in the analysis (the temporal coverage of Landsat and the spatial resolution of MODIS, in particular). So, how useful are these data and how robust is the shoreline identification when comparing data from different instruments and different times? Figure 3a shows a comparison of the shoreline during relatively high tide (1.3 m above mean water level at Anchorage), as obtained from Landsat in July in 1989 and in 2002. Despite of the 13 years difference, the shorelines are almost identical, except small differences near the edges of the inlet where mudflats are found (at the end of the two arms and south of Anchorage). The strong tidal velocities in the inlet (up to  $5 \text{ m s}^{-1}$  tidal bores [see Oey *et al.*, 2007]) are likely to change the morphology of the inlet by moving the sediment and changing the shoreline over long time. However, the very close proximity of the two shorelines in Figure 3a indicates that the shoreline identification method is quite robust.

[10] To evaluate how the different satellites and resolution affect the results, a comparison between Landsat and MODIS data are shown for low (Figure 3b) and high (Figure 3c) water level cases. During low tide (Figure 3b) there seems to be considerable differences between the Landsat and MODIS data. This discrepancy can be attributed to the MODIS lower pixel resolution (250–500 m) compared with the Landsat resolution (30–60 m). Because of the small-scale changes of water coverage (Figure 2), when a large pixel in MODIS is part water, part wet mud and part exposed land, the analysis can not definitely identify it as water, and thus creating a bias

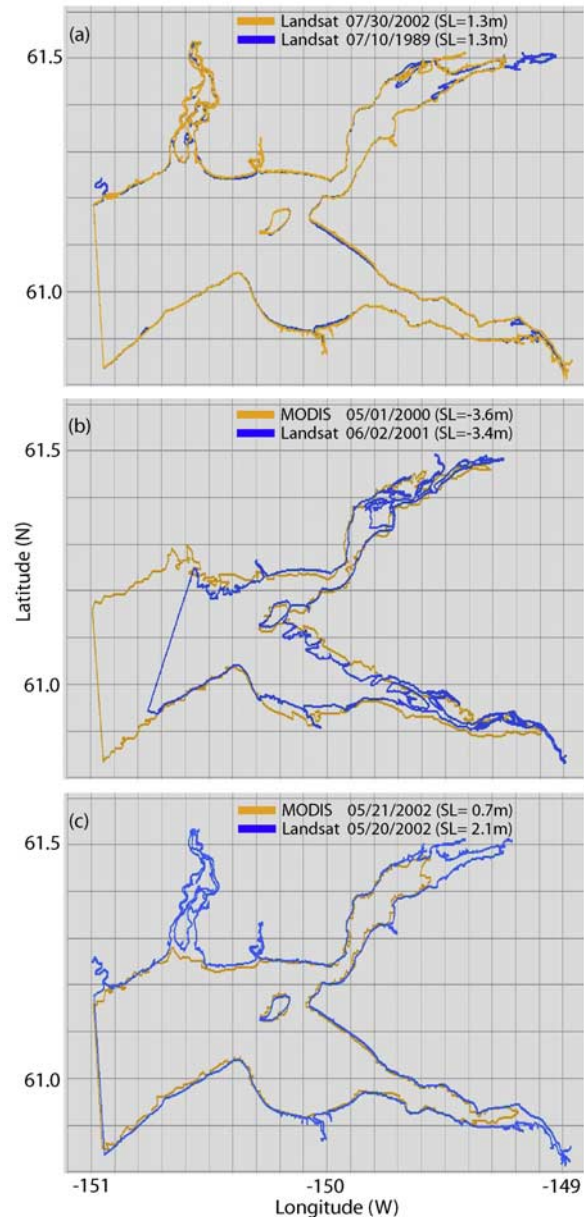


**Figure 3.** Comparisons between shoreline derived from different satellite images: (a) two Landsat data with similar sea level, but separated by 13 years, (b) Landsat data vs. MODIS data at low tide, and (c) Landsat data vs. MODIS data at high tide above mean sea level. The dates and sea level at Anchorage are indicated in each plot.

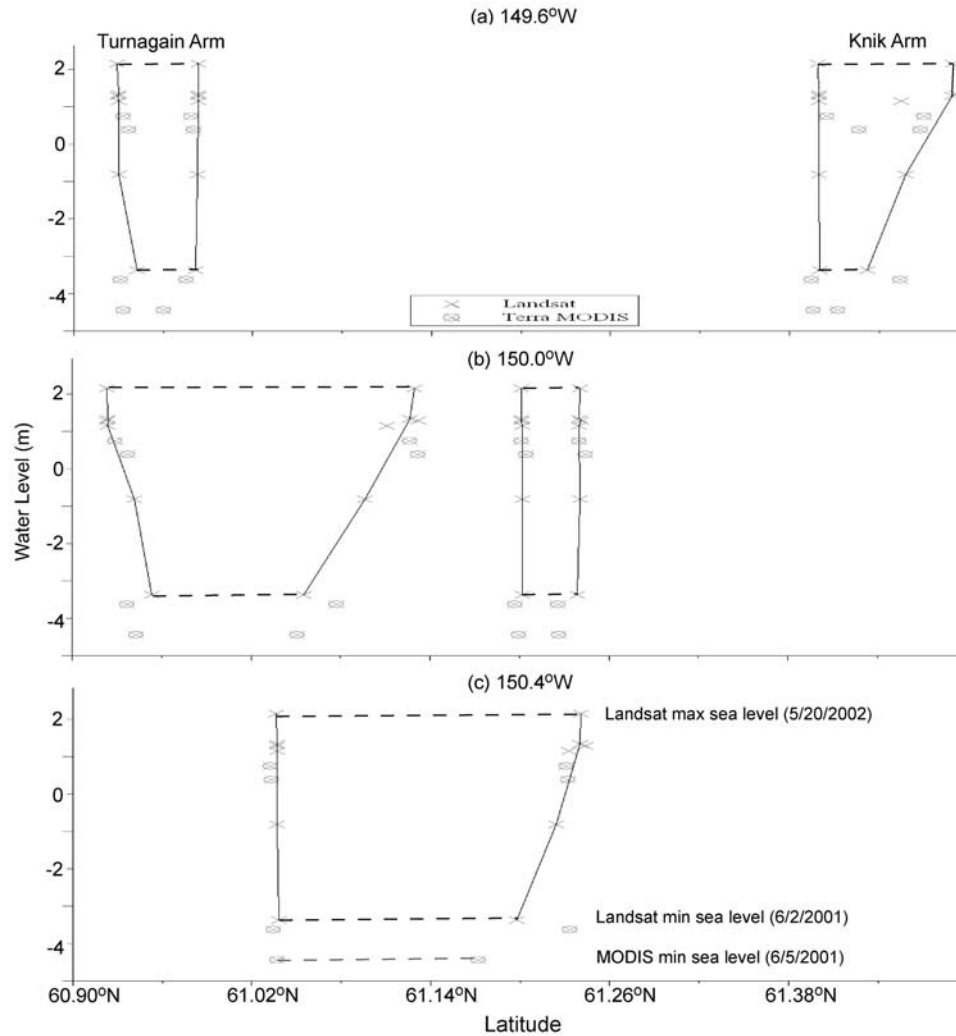


**Figure 4.** Three north-south cross sections of bottom topography derived from all the satellite images: (a) east of Anchorage at 149.6°W, (b) over Anchorage at 150.0°W, and (c) west of Anchorage at 150.4°W (the two Arms merged into one). Each point indicates the water-edge shoreline location (x-axis) and the Anchorage sea level at that time (y-axis). Solid lines and crosses are estimated topographies based on the best data points from Landsat, and circles with crosses are points from MODIS.

in having less water in MODIS compared with the higher resolution Landsat. During high tide, the differences between the two satellites are somewhat smaller (Figure 3c), as distinction between water and dry land is easier to identify than water and wet mud. Note however, that the highest water level images found here for the two satellites are not exactly at the same water level, thus there are differences at the ends of the two arms.

[11] The ten satellite-derived shorelines are associated with ten different tidal stages (Table 2). Assuming that in the vicinity of Anchorage the spatial variations of sea level at the time of each image are relatively small (compared with the 8–10 m tidal range), the shoreline data are matched with the corresponding Anchorage water level of each image. To demonstrate how the remote sensing data is converted into topographic maps, first, the vector shorelines derived from all image are described by  $[X(t), Y(t)] = [(X_i^n, Y_i^n), i = 1, 2, \dots, I; n = 1, 2, \dots, N]$ , where  $X$  and  $Y$  are longitude and latitude,  $N$  is the number of images (each at a different time  $t$ ) and  $I(n)$  is the number of shoreline points for each image. Then, by

matching each point with its water level we get a map of the shoreline elevation  $h(x, y, t)$ , or in a discrete form  $h(X_i^n, Y_i^n)$ , i.e.,  $N \times I(n)$  coastal height data points. Examples of topographic cross sections near Anchorage when taking  $h$  from the Anchorage sea level data are shown in Figure 4. The MODIS and Landsat are separated because of the bias discussed before. Except a couple of points, a consistent monotonic coastal topography is obtained from each satellite, demonstrating that the method can provide valuable coastal slope topography. Note that there are no direct observations of the mudflats topography to compare with, but as will be discussed next, the data provided by the remote sensing analysis seem more accurate than the limited topographic data that was previously available when the model was first constructed.

#### 4. Discussion

[12] This study demonstrates that publicly available remote sensing imagery can provide a reliable method to

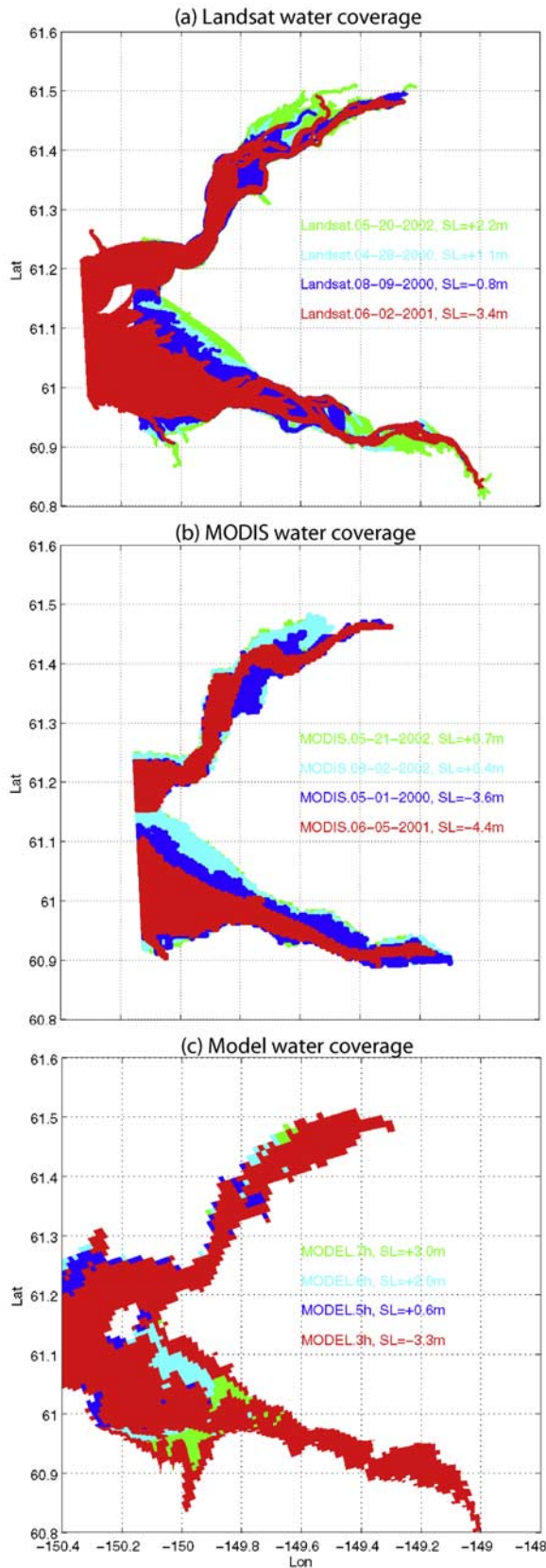


**Figure 5.** Water coverage at four different tidal stages (from low sea level, green, to high, red); the indicated height is the sea level at Anchorage. (a) Landsat, (b) MODIS and (c) inundation model.

improve mapping and prediction of tidal flood regions in Cook Inlet, Alaska (or in other regions where high resolution data from airborne LiDAR are not available). However, the remote sensing limitations in spatial (especially MODIS) and temporal (especially Landsat) resolutions require an innovative approach that combines available satellite data from different times and years with sea level data from observations and from model simulations. Landsat data should be preferred over MODIS for their higher spatial resolution, though more images than those used here are needed. Plans are underway to combine in the future as many satellite images as possible, including higher resolution remote sensing data, like SPOT satellite images with 2.5 m spatial resolution, that could be used to validate the coastlines estimated from lower resolution images like the Landsat and MODIS data. The method to match remote sensing-based shoreline data with water level data was demonstrated here using the sea level observations at Anchorage (Figure 4). However, plans are underway now to extend the analysis for regions farther away from Anchorage, whereas sea level from the model itself will be used to account for the spatial variations due to the time it takes for the tide to propagate the entire length of the shallow arms of the inlet.

[13] Can the analysis be used to evaluate model predictions and improve the model topography? Figure 5 compares the model water coverage (Figure 5c) at four different tidal stages with the Landsat (Figure 5a) and MODIS (Figure 5b) water coverage. It is clear that the lack of reliable topography data in the upper inlet when the inundation model was first constructed limits the model's ability to provide accurate flood predictions. Note, however, that other dynamic aspects such as tidal bores and rip currents are well simulated as shown by *Oey et al.* [2007]. The new information provided by the remote sensing data would thus be extremely useful to construct a new high resolution inundation model, though details of such plans are beyond the scope of this paper. This study is a proof of concept demonstration that can be implemented in other regions where high resolution topography data from direct observations are not available. Inundation models of storm surge and tsunamis can also be evaluated by remote sensing data as demonstrated here.

[14] **Acknowledgments.** The Cook Inlet inundation model was originally developed by L. Oey and his group at Princeton University with support provided by the Mineral Management Service. T.E. is supported by NSF as part of the Climate Process Team project and by NOAA's National Marine Fisheries Service. H.L. was partly supported by a grant to T.E. from ODU's Office of Research.

## References

- Ezer, T., R. Hobbs, and L.-Y. Oey (2008), On the movement of beluga whales in Cook Inlet, Alaska: Simulations of tidal and environmental impacts using a hydrodynamic inundation model, *Oceanography*, 21(4), 186–195.
- Hu, C., F. E. Muller-Karger, C. Taylor, K. L. Carder, C. Kelble, E. Johns, and C. A. Heil (2005), Red tide detection and tracing using MODIS fluorescence data: A regional example in SW Florida coastal waters, *Remote Sens. Environ.*, 97(3), 311–321.
- Kowalik, Z., W. Knight, T. Logan, and P. Whitmore (2006), The tsunami of 26 December, 2004: Numerical modeling and energy considerations, *Pure Appl. Geophys.*, 164, 1–15.
- Olmanson, L. G., M. E. Bauer, and P. L. Brezonik (2008), A 20-year Landsat water clarity census of Minnesota's 10,000 lakes, *Remote Sens. Environ.*, 112(11), 4086–4097.
- Oey, L.-Y., T. Ezer, C. Hu, and F. Muller-Karger (2007), Baroclinic tidal flows and inundation processes in Cook Inlet, Alaska: Numerical model-

ing and satellite observations, *Ocean Dyn.*, 57, 205–221, doi:10.1007/s10236-007-0103-8.

Zhou, G. (2009), Coastal 3D morphologic change analysis using LiDAR series data: A case study of Assateague Island National Seashore, *J. Coastal Res.*, in press.

---

T. Ezer, Center for Coastal Physical Oceanography, Old Dominion University, Norfolk, VA 23529, USA. (tezer@odu.edu)

H. Liu, Department of Political Science and Geography, Old Dominion University, Norfolk, VA 23529, USA.